

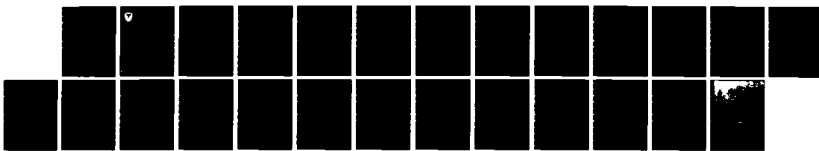
AD-A132 362 A VERTICAL WIND ANGLE STANDARD DEVIATION CALCULATION 1/1  
METHOD FOR THE UNSTABLE SURFACE BOUNDARY LAYER(U) ARMY  
DUGWAY PROVING GROUND UT C BILTOFT AUG 83

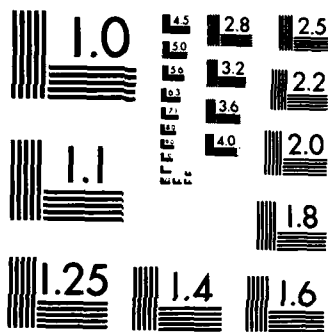
UNCLASSIFIED

DPG-TR-83-401

F/G 4/2

NL





MICROCOPY RESOLUTION TEST CHART  
NATIONAL BUREAU OF STANDARDS-1963-A

(2)



AD

TECOM Project No. 7-CO-RD3-DP1-008

DPG Document No. DPG-TR-83-401

ADA132362

A VERTICAL WIND ANGLE STANDARD DEVIATION CALCULATION  
METHOD FOR THE UNSTABLE SURFACE BOUNDARY LAYER

RESEARCH REPORT

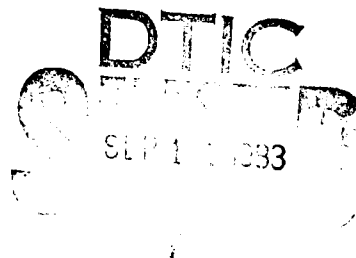
BY

CHRISTOPHER BILTOFT

AUGUST 1983

U.S. ARMY DUGWAY PROVING GROUND

DUGWAY, UTAH 84022



APPROVED FOR PUBLIC RELEASE: DISTRIBUTION UNLIMITED

83 09 13 058

DTIC FILE COPY

## TABLE OF CONTENTS

	<u>Page</u>
ABSTRACT.....	ii
1. SUMMARY.....	1
2. INTRODUCTION.....	1
3. PURPOSE.....	2
4. SYMBOLS.....	2
5. BACKGROUND.....	3
6. DISCUSSION.....	6
7. METHOD.....	8
8. VERIFICATION.....	10
9. CONCLUSIONS.....	13
10. LIMITATIONS.....	14
11. RECOMMENDATIONS.....	15
APPENDIX A - REFERENCES.....	A-1
APPENDIX B - PROGRAM.....	B-1
APPENDIX C - DISTRIBUTION LIST.....	C-1

Accession For	
NTIS GRA&I	<input checked="" type="checkbox"/>
DTIC TAB	<input type="checkbox"/>
Unannounced	<input type="checkbox"/>
Justification	<input type="checkbox"/>
By _____	
Distribution	
Available Other Copies	
Print _____	
A	



## 1. SUMMARY

Significant progress has been made over the last several decades towards the description and understanding of atmospheric turbulence, particularly in the unstable surface boundary layer. Much of this progress is due to the development of similarity theory arguments first postulated by the Soviet scientist Obukhov in 1946. This report is an introduction to basic similarity theory arguments and the application of the theory to practical problems in diffusion. It is intended to assist individuals with only a passing acquaintance with diffusion theory in the planning and execution of diffusion and hazard studies.

A fundamental diffusion problem is the dilution that results from turbulent vertical cloud growth. Vertical cloud growth is described by the standard deviation of the vertical distribution of cloud material ( $\sigma_z$ ). Estimates of  $\sigma_z$  are frequently obtained from Pasquill-Turner (P-T) stability categories. Sigma z can also be calculated as the product of travel distance ( $x$ ) and the standard deviation of the vertical wind angle ( $\sigma_e$ ). An explicit functional relationship between  $\sigma_e$  and the stability parameter  $z/L$ , where  $z$  is height and  $L$  is the characteristic length, is derived from similarity theory. This functional relationship is verified on a set of precisely measured micrometeorological field data. The performance of similarity theory  $\sigma_e$  calculations and P-T estimates is subsequently tested using  $\sigma_e$  data collected at DPG. The similarity theory computations are shown to be substantially superior to the P-T  $\sigma_e$  estimates. Adoption of similarity theory arguments should materially improve Army testing and hazard prediction efforts involving atmospheric diffusion and transport processes.

## 2. INTRODUCTION

Sigma z is a measure of the vertical dilution in a diffusing cloud caused by turbulent motions. Diffusion calculations are critically dependent on an accurate specification of  $\sigma_z$ . In diffusion models  $\sigma_z$  is usually specified as the product of travel distance ( $x$ ) and  $\sigma_e$ , where  $\sigma_e$  is a measure of the rate of vertical mixing (turbulence). Sigma e is defined as the vertical wind angle standard deviation. DPG uses bi-directional wind vanes (bivanes) to measure the wind angles from which  $\sigma_e$  is calculated.

When measured wind angle data are unavailable,  $\sigma_z$  estimates can be obtained from stability categories. A fixed value of  $\sigma_e$  is implied for each category. Pasquill (1961) introduced the most widely used set of stability categories. Turner (1964) modified the Pasquill method so that sun elevation angle, wind speed, and cloud cover can be used to determine the stability category. The Pasquill-Turner (P-T) method is popular because it requires a minimum of meteorological data and a simple set of look-up tables to arrive at an estimate of  $\sigma_z$ . The P-T method is widely used for hazard calculations. It is also used to categorize stability for smoke diffusion trials and as a go/no-go test criterion.

An alternative to direct  $\sigma_e$  measurement or stability category estimates for diffusion problems within the surface boundary layer (SBL) is presented in this report. The SBL is the thin layer of air extending several tens of meters above the earth's surface. Turbulent motions within the SBL are determined by fluxes, that is rate of transfer of momentum (represented by shear

stress,  $\tau$ ) and heat ( $F_h$ ). Shear stress and heat flux are not directly measured at DPG because high-frequency instrumentation is unavailable. These fluxes may be calculated, however, using gradients obtained from profile measurements of wind speed and temperature. It is therefore possible, under certain conditions, to specify turbulent motions within the SBL as a function of appropriate combinations of these gradients.

Similarity theory rises from the fact that within the first several tens of meters above ground level there exists a set of characteristic parameters with units of length, velocity, and temperature which are essentially invariant with height. These characteristic parameters define the SBL as a layer of nearly constant stress and heat flux. Monin and Obukhov (1954) used dimensionless combinations of these characteristic parameters to describe the SBL. Of principal importance in this report is the characteristic length ( $L$ ). The dimensionless ratio of height ( $z$ ) to  $L$  forms the fundamental stability property of the SBL. Consequently, SBL turbulence can be described as a function of  $z/L$ , using similarity theory arguments originated by Obukhov in 1946 (see Obukhov, 1971), and sigma  $\epsilon$  can be calculated from measured gradients of wind and temperature.

### 3. PURPOSE

The purpose of this report is to derive the stability parameter  $z/L$  as an explicit function of measureable wind and temperature gradients and to apply  $z/L$  to the calculation of  $\sigma_e$ .

### 4. SYMBOLS

$c_p$	specific heat at constant pressure (calories gram <sup>-1</sup> degree <sup>-1</sup> )
$E$	evaporation fraction, the ratio $F_l/(F_l + F_h)$ (dimensionless)
$FE$	fractional error (dimensionless)
$FE_{rms}$	root mean square fractional error (dimensionless)
$f$	Coriolis parameter (second <sup>-1</sup> )
$F_g$	heat flux into the ground (milliwatts meter <sup>-2</sup> )
$F_h, F_l$	sensible heat and latent heat (milliwatts meter <sup>-2</sup> )
$F_s$	flux of substances (variable dimensions)
$k$	von Karman's constant (dimensionless)
$K_h, K_m$	eddy diffusivity for heat and momentum (meters <sup>2</sup> second <sup>-1</sup> )
$K_s$	eddy diffusivity for unspecified substances (meters <sup>2</sup> second <sup>-1</sup> )
$L$	Obukhov length (meters)
$\ell$	mixing length (meters)

>	pressure (millibars)
R	net radiation (milliwatts meter <sup>-2</sup> )
Ric	critical Richardson number (dimensionless)
S	a generalized property in the air (variable dimensions)
S*	a scale with dimensions of S
$\bar{T}$	time-averaged temperature at a specific height (degrees Kelvin)
$\bar{u}$	time-averaged wind speed at a specific height (meter second <sup>-1</sup> )
u,v	wind speed along the x, y axis (meters second <sup>-1</sup> )
z	height of measurement (meters)
$z_0$	roughness length (meters)
$\alpha$	ratio of $K_h$ to $K_m$ (dimensionless)
$\varepsilon_s, \varepsilon_b$	rates of turbulent energy addition by shearing and buoyancy forces (meters second <sup>-3</sup> )
$\theta$	potential temperature (degrees Kelvin)
$v^*$	friction velocity (meters second <sup>-1</sup> )
$\rho$	density (grams centimeter <sup>-3</sup> )
$\sigma_e$	vertical wind angle standard deviation (degrees or radians)
$\sigma_w$	square root of variance in vertical wind velocity (meters second <sup>-1</sup> )
$\sigma_z$	standard deviation of vertical distribution of diffusing material (meters)
$\tau$	shear stress (gram centimeter <sup>-1</sup> second <sup>-2</sup> )
$\phi_m, \phi_h$	dimensionless wind shear and temperature gradient
$\phi_s$	dimensionless universal function of stability
$\psi$	diabatic influence function (dimensionless)

## 5. BACKGROUND

The Reynolds number is a dimensionless number expressing the ratio of inertial to viscous forces in a moving fluid. When the Reynolds number is large, flow is considered to be fully turbulent. This equates to thorough mixing within the fluid. The assumption of a large Reynolds number through the SBL permits a description of turbulent processes within this layer using semi-empirical equations developed from fluid dynamics laboratory experiments.

Turbulent motions in a fluid cause the net movement of a diffusing material down a gradient at a rate proportional to the gradient. The relationship of the flux of a diffusing material to its gradient is described by a semi-empirical gradient transfer equation, equation (1).

$$F_S = -\rho K_S (\partial S / \partial z) \quad (1)$$

The gradient transfer equation describes the flux ( $F_S$ ) of substance S as a function of density ( $\rho$ ), its eddy diffusivity ( $K_S$ ) which specifies the rate of turbulent mixing, and the vertical gradient of S ( $\partial S / \partial z$ ). For heat, this equation becomes

$$F_h = -\rho K_h c_p (\partial \theta / \partial z) \quad (2)$$

where  $F_h$  is the sensible heat flux,  $K_h$  is thermal diffusivity,  $c_p$  is specific heat at constant pressure, and  $\partial \theta / \partial z$  is the lapse rate (gradient) of potential temperature.

Classical mixing length theory describes the flux to gradient relationship for momentum, with equation (3).

$$\tau = \rho \ell^2 (du / dz) |du / dz| \quad (3)$$

Equation (3) presents  $\tau$  in fluid flowing past a stationary boundary as a function of velocity gradient and a mixing length ( $\ell$ ) proportional to distance from the boundary. Separation of  $du / dz$  terms allows equation (3) to satisfy the requirement that  $\tau$  changes sign with  $(du / dz)$ . From equations (1) and (3), eddy diffusivity for momentum ( $K_m$ ) takes the form

$$K_m = \ell^2 (du / dz) \quad (4)$$

Eddy and thermal diffusivity have identical signs and units. The ratio  $K_h / K_m$  is a function of stability and is represented by  $\alpha$ .

$$K_h / K_m = \alpha \quad (5)$$

The ratio of  $\tau$  to density is conveniently represented by friction velocity ( $v_*$ ), as defined by equation (6).

$$v_*^2 = \tau / \rho \quad (6)$$

Then equation (3) can be expressed in terms of  $v_*$ , as in equation (7).

$$v_*^2 = \ell^2 (du / dz) |du / dz| = K_m |du / dz| \quad (7)$$

The heat flux equation (equation 2) can be further simplified, using equation (5) to eliminate  $K_h$  and equation (7) to eliminate  $\ell^2$  in favor of  $v_*^2$ . The result is equation (8), which describes heat flux as a function of measureable potential temperature and wind speed gradients.

$$F_h = -\alpha \rho c_p v_*^2 (\partial \theta / \partial z |du / dz|) \quad (8)$$

It is necessary to measure wind and temperature over identical time and height intervals for the gradients used in equation (8) and all subsequent gradient equations.

Based on dimensional arguments, Monin and Obukhov (1954) introduced the general relationship

$$dS/dz = S^* \phi_S / kz \quad (9)$$

where  $S$  is the mean amount of a property in a unit mass of air and  $S^*$  is a characteristic scale with dimensions of  $S$  and defined by  $F_S/\rho v^*$ . The variable  $\phi_S$  is a dimensionless universal function of stability which assumes a value of unity for neutral conditions. The von Karman constant ( $k$ ) is a constant of proportionality (see Businger, 1973). For wind speed gradient, equation (9) becomes

$$du/dz = v^* \phi_m / k(z+z_0) \quad (10)$$

Roughness length ( $z_0$ ) is introduced into equation (10) to prevent infinite shear at the surface. This equation is therefore used only for  $z > z_0$ . The term  $\phi_m$  is a dimensionless wind shear [see equation (21) for an empirical expression of  $\phi_m$ ].

Integration of equation (10) yields the logarithmic wind profile, equation (11).

$$\bar{u}/v^* = (\ln((z+z_0)/z_0) - \psi)/k \quad (11)$$

The magnitude of  $z_0$ , <0.1 m for open fields, is sufficiently small enough that it is usually ignored in the numerator of equation (11). The diabatic influence function ( $\psi$ ) accounts for the effects of thermal stratification on the wind profile. Equation (12) presents the unstable case diabatic influence function was derived as a unique function of  $\phi_m$  by Paulson (1970).

$$\psi = 2\ln((1+\phi_m^{-1})/2) + \ln((1+\phi_m^{-2})/2) - 2\tan^{-1}\phi_m^{-1} + \pi/2 \quad (12)$$

Obukhov (1971) reasoned that the mean turbulence in the SBL is determined by only four parameters: density, a buoyancy parameter ( $g/T$ ), turbulent shear stress, and vertical heat flux. These four parameters combine to form the Obukhov length ( $L$ ), equation (13).

$$-L = c_p \rho T v^* / kg F_h = c_p \rho T \tau^{3/2} / kg \rho^{1/2} F_h \quad (13)$$

The sign of  $L$  is chosen so that  $L$  is negative for unstable thermal stratification. Hereafter in this report, the Obukhov length proceeded by a minus sign ( $-L$ ) implies heat flux directed away from the surface, and a lapse of potential temperature. With  $c_p$ ,  $\tau$ ,  $k$ ,  $g$ , and  $F_h$  remaining more or less constant,  $-L$  will decrease with height as  $T/\rho^{1/2}$ . Because the lapse of  $T/\rho^{1/2}$  over a few tens of meters of height is a small fraction of the absolute surface value,  $-L$  also remains nearly constant within the SBL. The Obukhov length has units of meters. Therefore  $z/-L$  is dimensionless. Obukhov intended for a ratio of  $z/-L$  equal to unity to imply a balance between buoyant energy production and shear production, and defined  $L$  as the height of the sub-layer of dynamic turbulence. It is shown below that this balance is actually achieved at a considerably smaller value of  $z/-L$ .

Because it depicts the relative contributions of the buoyancy term, heat flux, and shear stress to turbulence,  $z/L$  functions as a dimensionless stability parameter. When buoyant forces are negligible and  $F_h$  is small, the magnitude of  $-L$  is large with respect to any height within the SBL, and  $z/L$  is close to zero. Turbulence for this condition is mechanical, or generated by air blowing over roughness elements. As the ground is heated,  $F_h$  assumes a nonnegligible value and buoyant forces make a contribution to turbulence. Monin and Yaglom (1971) found buoyancy effects contributing to turbulence as  $z/L$  exceeded 0.03. With increasing  $F_h$  (or increasing  $z$  with constant  $F_h$ ), buoyancy increases until the point is reached where turbulence production due to buoyancy and shear forces is in balance. This occurs as  $z/L$  approaches 0.36. When  $z/L$  increases beyond 0.36, buoyancy becomes progressively more dominant until a state of windless convection is reached. Windless convection, characterized by intense surface heating with light and variable winds, is the condition where shear production and mechanical turbulence effects are negligible. This condition appears as  $z/L$  approaches 1.0.

## 6. DISCUSSION

Before specifying the flux-gradient relationship to turbulence with the use of  $z/L$ , some underlying assumptions must be investigated. Both similarity theory and P-T  $\sigma_e$  estimates depend on the magnitude of surface roughness. Roughness effects are specified by the ratio of height to roughness length,  $\ln(z/z_0)$  in equation (11). For an open field with roughness of a few centimeters, a factor of 2 change in roughness causes a variation in  $u/v^*$  of 10 to 15 percent and a comparable change in turbulence. Therefore, small-scale changes in roughness have only a minor effect on diffusion. This is fortunate because roughness is often difficult to specify precisely. However, an abrupt change in roughness, due to placement of obstacles in the flow, can have a significant effect on turbulence. At a given site, roughness may vary with wind azimuth angle, due to wind fetch over roughness elements of different size. Roughness may also vary with wind speed; at higher wind speeds some vegetation bends to reduce drag. When wind blowing over a homogeneous surface encounters an abrupt change in roughness, a new sublayer of turbulence develops. Turbulence characteristics within this sublayer reflect the influence of the new surface roughness. Elliott (1958) described the height of this new sublayer with the empirical equation

$$h_{\text{new}} = 0.86 \times 0.8 z_0^{0.2} \quad (14)$$

For equation (14),  $z_0$  is the roughness of the new surface,  $x$  is the downwind distance from the discontinuity, and  $h_{\text{new}}$  is the height of the top of the new sublayer. For an obstacle generating a new roughness of 0.1 m placed 100 m upwind of a meteorological tower,  $h_{\text{new}}$  will be 21.6 m. Instruments on the tower below this level will measure turbulence due to the new roughness regime while above this level the old roughness regime predominates. Portions of a diffusing cloud passing through different roughness regimes will diffuse at different rates, vastly complicating attempts to analyze or predict cloud behavior.

The P-T categories are set up for a site roughness of a few centimeters. For maximum accuracy, median turbulence values for each P-T category should be established using meteorological measurements at each site where P-T categories are used. This was done at DPG by Waldron (1977). Changes in roughness are accommodated by equation (11) for similarity theory. For diffusion

tests, it is highly desirable to avoid drastic changes in roughness with the resultant formation of multiple roughness sublayers.

The similarity and P-T methods both rely on the assumption of constant stress in the SBL to produce reasonable turbulence estimates. Validity of the constant  $\tau$  assumption is examined using an equation of motion.

$$\frac{\partial \tau_{xz}}{\partial z} = \rho du/dt + \frac{\partial P}{\partial x} - \rho fv \quad (15)$$

Equation (15) describes the lapse of  $\tau$  in the xz plane. An analogous expression can be written for  $\tau$  in the yz plane. Terms on the right side of equation (15) include the time rate of wind speed change ( $du/dt$ ) in the alongwind (x) direction, the x component of pressure gradient ( $\partial P/\partial x$ ), and the Coriolis term ( $\rho fv$ ) where  $f$  is the Coriolis parameter and  $v$  is the crosswind component of wind speed. For quasi-geostrophic balance,  $\partial P/\partial x$  is in rough equilibrium, with  $\rho fv$ . The  $\tau$  gradient is therefore governed largely by the magnitude of alongwind acceleration ( $du/dt$ ).

For similarity method computations, stress is assumed to be nearly constant when  $\tau$  at a given height is within 20 percent of its surface value,  $\tau_0$ . For  $v^* = 50$  cm/sec and density at a constant value of  $0.0012$  g/cm $^3$ , equation (6) yields  $\tau_0 = 3.0$  g/cm sec $^2$ . A strongly accelerating wind, with 6 m/sec speed change within 10 minutes, produces a  $du/dt$  of 1.0 cm/sec. From equation (15), this acceleration would produce a  $\Delta\tau$  of 0.6 g/cm sec $^2$  (20 percent of  $\tau_0$ ) at a height of 5.0 m. For a more typical wind speed change of 1.0 m/sec in 10 minutes, stress remains within 20 percent of  $\tau_0$  for 30 m. With extremely low wind speeds, as expected in windless convection,  $v^*$  may be 10 cm/sec and  $\tau_0$  may be only 0.12 g/cm sec $^2$ . Then, a 1.0 m/sec wind speed change in 10 minutes will produce a stress deviating 20 percent from  $\tau_0$  in 1.2 m. Therefore, the constant  $\tau$  assumption is valid for several tens of meters above the surface when accelerations are modest and  $v^*$  is moderately large. In a rapidly accelerating wind field, or a windless convection regime with light and variable winds, the constant stress can be violated within a few meters of the surface. Fortunately, large sustained accelerations in the wind are not likely except in the presence of convective storms. Erratic results can also be expected when light winds and intense surface heating persist.

Assumptions regarding fluxes of heat and moisture are treated differently by the P-T and similarity methods. The P-T method assumes a constant functional relationship between net solar radiation ( $R$ ) and  $F_h$ .

Net radiation,  $F_h$ , latent heat flux ( $F_l$ ), and flux of heat into the ground ( $F_g$ ) are related by equation (16).

$$R - F_g = F_l + F_h \quad (16)$$

Swinbank (1964) tabulated  $R$  and  $F_g$  data taken at an open field near Kerang, Australia under a variety of weather conditions. These data show  $F_g$  to be approximately 20 percent of  $R$ , with the ratio holding fairly constant at that site. Changes in the  $F_g/R$  ratio could be expected for different ground cover or soil types, but no comprehensive evaluation of this phenomenon is available.

Dyer (1961) defined evaporation fraction ( $E$ ) as the ratio of  $F_l$  to  $F_l + F_h$ , as in equation '17)

$$E = F_l / (F_l + F_h) \quad (17)$$

Dyer's data show that E varies from 0.7 following a rain event to 0.3 on a dry day. Consequently, variations from the assumed relationship between R and  $F_h$  can be as large as  $\pm 40$  percent.

Because similarity relationships do not rely on constancy of the ratio  $F_h/(R-F_g)$ , the effects of moisture variability are considerably less severe. Dyer and Hicks (1970) accounted for latent heat effects on L by modifying equation (13) into equation (18).

$$-L = c_{pp} T v^*^3 / kg (F_h + 0.07 F_l) \quad (18)$$

Equation (18) shows that, for the maximum value of  $F_l$  where the ratio of  $F_h/F_l$  is 3/7, the contribution of  $F_l$  is only 16 percent of  $F_h$ . If available, the  $F_l$  factor should be considered in length scale computation, but omission would generally result in an error of 16 percent or less (except over very wet surfaces).

Another implied assumption required to obtain reasonable estimates of  $\sigma_e$  is that fluxes remain relatively invariant with respect to time. Profiles of temperature and wind speed adjust slowly to changes in the fluxes of these parameters. Dyer (1963) calculated the time required for profiles to reach 90 percent adjustment to the new condition following an abrupt change in surface flux. The time required was 14 minutes for profiles to stabilize with the new condition to a height of 10 m, and 30 minutes to a height of 20 m. He concluded that careful selection of meteorological conditions, particularly with respect to insolation and wind fields, is necessary to satisfy the steady state assumption implicit in all flux-gradient considerations.

## 7. METHOD

When site and meteorological conditions satisfy the assumptions discussed in the previous section, flux-gradient relationships can be used to calculate  $z/L$ . The flux form of the stability parameter is expressed by equation (19).

$$z/L = -kgF_hz/\rho c_p \bar{T} v^*^3 \quad (19)$$

Equation (19) can be transformed into profile form for the unstable case by introducing equation (8) for  $F_h$  and equation (11) for  $v^*$ . After simplification, the result is equation (20).

$$z/-L = -\alpha g z (\partial \theta / \partial z) [du/dz] [\ln(z/z_0) - \psi] / \bar{T} \bar{u} \quad (20)$$

Equation (20) has several advantages as a means of describing stability in the SBL. First, equation (20) does not require specification of k. The absolute value of von Karman's constant is not precisely known (see Businger, 1973); accepted values range from 0.34 to 0.41. Second, equation (20) does not contain higher order terms, such as  $(du/dz)^2$  as found in some other stability parameters. Gradients of wind and temperature are small, often the same order of magnitude as the least significant digit in the profiles from which they are computed. Using gradients as higher order terms magnifies the potential error. Accuracy of the gradient measurements required in equation (20)

represent the largest source of error in the expression. This is discussed further in Verification (Part 8) below.

Equation (20) contains two terms,  $\alpha$  and  $\psi$ , which require further specification as functions of  $z/-L$ . The term  $\alpha$  (the ratio of thermal to eddy diffusivity) is identified by Businger et al. (1971) as the ratio  $\phi_m/\phi_h$ . Businger, et al. established empirical relationships between  $\phi_m$ ,  $\phi_h$ , and  $z/-L$  as presented in equations (21) and (22).

$$\phi_m = (1 + 15z/-L)^{-1/4} \quad (21)$$

$$\phi_h = 0.74(1 + 9z/-L)^{-1/2} \quad (22)$$

Then  $u$  can be expressed as a function of  $z/-L$ , as in equation (23).

$$u = 1.35(1 + 9z/-L)^{1/2}/(1 + 15z/-L)^{1/4} \quad (23)$$

With  $\phi_m$  described above as a function of  $z/-L$ ,  $\psi$ , given by equation (12) as a function of  $\phi_m$ , is also a function of  $z/-L$ . With  $\alpha$  and  $\psi$  specified as functions of  $z/-L$ , a simple convergence scheme allows for rapid computer solutions of  $z/-L$  from equation (20) using wind and temperature gradient data (Appendix B).

With  $z/-L$  determined from measured wind and temperature profiles, it is possible to move towards a similarity theory solution for  $\sigma_e$ . Sigma e is approximated by the ratio of  $\sigma_w$  (the square root of the variance in vertical wind velocity) and  $u$  as in equation (24).

$$\sigma_e \approx \sigma_w/u \quad (24)$$

Panofsky and McCormick (1960) assumed that  $\sigma_w$  is determined by  $z$  and the rates of turbulent energy addition by shearing ( $\epsilon_s$ ) and buoyant ( $\epsilon_b$ ) forces, as in equation (25).

$$\sigma_w = A[z(\epsilon_s + B\epsilon_b)]^{1/3} \quad (25)$$

$A$  and  $B$  in equation (25) are constants to be determined below. Pasquill (1974) defines  $\epsilon_s$  and  $\epsilon_b$  as follows:

$$\epsilon_s = v^2 du/dz \quad (26)$$

$$\epsilon_b = gF_h/\rho c_p T \quad (27)$$

Equation (13) can be used to simplify equation (27), producing equation (28).

$$\epsilon_b = -v^3/Lk \quad (28)$$

Equation (10) is then used to eliminate  $v^2$  from equations (26) and (28). Equation (26) becomes equation (29), and the ratio  $\epsilon_s/\epsilon_b$  is given by equation (30).

$$\epsilon_s = k^2 z^2 (du/dz)^3 / \phi_m^2 \quad (29)$$

$$\epsilon_s/\epsilon_b = -L\phi_m/z \quad (30)$$

Equations (29) and (30) are then applied to equation (25). After some algebraic manipulation and division by  $v^*$ , the result is equation (31).

$$\sigma_w/v^* = Ak^{-1/3}(\phi_m + B(z/-L))^{1/3} \quad (31)$$

Following suggestions in Pasquill (1974), constants  $Ak^{-1/3}$  and  $B$  were assigned values of 1.3 and 1.73 respectively.

The dimensionless wind shear term in equation (31) is a slowly decreasing function of  $z/-L$ , whereas the buoyancy term ( $Bz/-L$ ) is an increasing function of  $z/-L$ . The combined effect of these terms is that  $\sigma_w/v^*$  remains nearly constant until  $z/-L$  reaches a value of 0.36. This is the equilibrium point where  $\phi_m$  equals 1.73  $z/-L$  and shear and buoyancy forces are in balance. Beyond this point, the buoyancy effect becomes dominant and  $\sigma_w/v^*$  increases rapidly with increasing  $z/-L$ . Using equation (21) for  $\phi_m$ , the working expression for  $\sigma_w/v^*$  is equation (32).

$$\sigma_w/v^* = 1.3((1 + 15z/-L)^{-1/4} + 1.73z/-L)^{1/3} \quad (32)$$

Equation (32), used in a ratio with the logarithmic wind profile [equation (11)], satisfies equation (24) and produces an estimate of  $\sigma_e$ .

$$\frac{\sigma_w/v^*}{\bar{u}/v^*} = \frac{1.3((1 + 15z/-L)^{-1/4} + 1.73z/-L)^{1/3}}{[\ln(z/z_0) - \psi]/k} = \sigma_w/\bar{u} = \sigma_e \quad (33)$$

Equation (33) describes  $\sigma_e$  as a function of stability parameter  $z/-L$ , height, and roughness. Following Businger (1973),  $k$  is assigned the value 0.35.

## 8. VERIFICATION

a. Kansas 1968 Field Program. The similarity method for  $\sigma_e$  computation developed in previous sections was written into a short computer program (Appendix B) and tested on Project Kansas field data (Izumi, 1971). This project was conducted in the summer of 1968 at a field site in southwest Kansas. The data include drag plate measurements of  $v^*$  and research grade wind and temperature profile measurements on a 32-m tower. Turbulence data at 5.66, 11.31, and 22.63 m were obtained using sonic anemometers. High frequency turbulent velocity fluctuations and air temperature fluctuations were measured 20 times per second at three levels concurrently with temperature and wind speed profile measurements. The basic sample averaging period was 15 minutes and sampling rate for slow response profile data was one per second. Equation (24) was used to obtain  $\sigma_e$  for each unstable case averaging period. Site roughness was 0.024 m. Gradients of wind speed and temperature were obtained from measured profiles by differentiating second order polynomials in  $(\ln z)$  fitted to measured values (Izumi, 1971).

Verification required comparison of "measured"  $\sigma_e$  obtained from the high frequency turbulence measurements with  $\sigma_e$  computed from gradients of the tower profile data via equations (20) and (33). Fractional error (FE), defined by equation (34), was used for verification.

$$FE = (\sigma_{e\text{comp}} - \sigma_{e\text{meas}})/_{1/2}(\sigma_{e\text{comp}} + \sigma_{e\text{meas}}) \quad (34)$$

Fractional error is the difference between observed and predicted  $\sigma_e$ , normalized by the average of observed plus predicted  $\sigma_e$ . FE computed in this way provides a logarithmically unbiased means of presenting the fractional difference between measured and computed parameter values. Mean FE is defined by equation (35).

$$FE = \sum FE/N \quad (35)$$

Fractional error is positive (negative) if the computed  $\sigma_e$  is greater (less) than the measured value. Root mean square fractional error (FErms) is defined by equation (36).

$$FErms = (\sum FE^2/N)^{1/2} \quad (36)$$

Results of the unstable case Kansas field data verification are in Table 1.

Table 1. Mean and Root Mean Square Fractional Error for Kansas 1969 Field Program Data (Reference 1) at Indicated Heights Above Ground Level.

Height (m)	Mean Measured $\sigma_e$	Mean Calculated $\sigma_e$	Mean FE	FErms	Number of Observations
5.66	5.51	5.35	-0.028	0.060	75
11.31	5.62	5.33	-0.048	0.090	75
22.63	5.83	5.55	-0.044	0.149	68

There is a slight tendency for underprediction of  $\sigma_e$ , as demonstrated by the negative values of mean FE in Table 1. Fractional errors were small for almost every run. At 5.66 m there were no cases of  $FE > 0.2$ . At 11.31 m there were two runs with  $FE > 0.2$  (2.7 percent), and at 22.63 m there were 11 runs with  $FE > 0.2$  (16 percent). In no run did the error approach a factor of 2, or  $FE = 0.67$ .

The FErms was less than .10 at the 5.66- and 11.31-m levels, but increased to nearly .15 at 22.63 m. This increase in error at 22.63 m was largely due to resolution of the gradients to only two significant digits beyond the decimal point. At 22.63 m, the gradients used for  $\sigma_e$  computations were the same order of magnitude as the least significant digit. Because of this gradient problem,  $-L$  was again computed using the 5.66 m gradients. This  $-L$  was assumed to remain constant through the surface boundary layer, and turbulence at 22.63 m was then re-computed using this constant  $-L$ . The result was a decrease in FErms from 0.149 to 0.125. In spite of the resolution difficulties, these data demonstrate the effectiveness of the similarity method turbulence computations with the SBL.

b. DPG Tower. Measurements obtained with research grade instruments, during carefully chosen meteorological conditions at a uniform site, demonstrated the potential accuracy for similarity method turbulence computations.

However, to be truly useful for diffusion calculations, a method must work under a wide variety of locations and meteorological conditions. For this reason, the effectiveness of the similarity and P-T  $\sigma_e$  computations methods were compared using turbulence measurements from a DPG meteorological tower where data were collected hourly over an eight-week period. These data consisted of turbulence, wind, and temperature profiles in 10-minute averages for every data collection hour at the DPG West Vertical Grid (Waldron, 1977). The sampling rate was one per second. Gradients of wind and temperature were taken from least squares fitted data. The turbulence measurements were obtained from bivanes. Kaimal et al. (1964) performed a comparison of bivane and sonic anemometer vertical turbulence component measurements. The bivane data were found to correspond well with the sonic data for the lower frequencies of turbulence expected during unstable lapse rates. Weather observations were also included with DPG tower data to allow computation of P-T categories.

Waldron (1968, unpublished technical report) used the West Vertical Grid tower data to relate  $\sigma_e$  values to each P-T category. The median  $\sigma_e$  for each category was obtained by dividing the recommended  $\sigma_z$  at 100 m by distance. The resultant  $\sigma_e$  in radians was then converted to degrees (Table 2) for use in the evaluation.

Table 2. Median 8.0-m Level  $\sigma_e$  Values for P-T Stability Categories from DPG West Vertical Grid Turbulence Measurements.

Stability Category	A	B	C	D	E	F
Median $\sigma_e$	15.5	10.08	6.7	4.5	2.98	2.0

Before evaluation of the P-T and similarity methods, the data in Waldron (1977) were quality checked. Systematic errors in the temperature profiles were present for approximately the last half of the data. This was probably caused by one or more of the temperature sensors drifting off calibration. Data containing systematic errors were eliminated, as were incomplete data records, leaving 139 unstable cases for evaluation. For tabulation, the data for each of the cases were grouped by the measured  $\sigma_e$  value. The results of verification at the 8.0-m level are presented in Tables 3 and 4.

The DPG tower results show fractional error, increasing with measured  $\sigma_e$  for both similarity and P-T methods. A consistent pattern of underprediction is also present with both methods. The similarity method was in error by  $|FE| > 0.2$  for 37 trials (27 percent of the total), while the P-T method posted an equivalent error level for 60 trials (43 percent). Four similarity method trial calculations were in error by a factor of two for a rate of 3 percent, versus 12 trials (9 percent) for the P-T method. Most of the large errors for both methods were due to underprediction.

Table 3. Mean Observed and Calculated DPG West Vertical Grid Turbulence Measurements for Indicated Measured  $\sigma_e$  Ranges.

Measured $\sigma_e$ Range	Number of Observations	Mean Observed $\sigma_e$	Mean Similarity $\sigma_e$	Mean P-T $\sigma_e$
<5.0	44	4.62	4.76	4.60
5.1 - 10.0	61	6.53	6.39	5.73
10.1 - 15.0	14	11.91	9.77	8.63
>15.1	20	21.6	18.15	10.39

Table 4. Mean and Root Mean Square Fractional Error for 8.0-M Level, DPG West Vertical Grid Turbulence Measurements for Indicated  $\sigma_e$  Ranges.

Measured $\sigma_e$ Range	Number of Observations	Similarity FE	Similarity FERms	P-T FE	P-T FERms
<5.0	44	0.029	0.080	-0.006	0.097
5.1 - 10.0	61	-0.040	0.189	-0.146	0.277
10.1 - 15.0	14	-0.134	0.396	-0.328	0.385
>15.1	20	-0.247	0.419	-0.689	0.724
All	139	-0.058	0.242	-0.198	0.357

## 9. CONCLUSIONS

DPG West Vertical Grid tower grid verification reveals that the P-T turbulence estimates are quite accurate for near-neutral values of  $\sigma_e$ , but that error increases with the magnitude of  $\sigma_e$ . This increase in error is due in part to the violation of the P-T method assumptions described in Section 6. A measurement of mean wind speed and an estimate of net radiation provide insufficient information for the accurate estimation of turbulence under diabatic conditions. Another source of inaccuracy is that the P-T method offers a choice of only six possible  $\sigma_e$  values, chosen to represent centroid turbulence values within each category. Turbulence occurs as a continuum and varies with height and time in response to shear and buoyancy forces. Any attempt to estimate turbulence using a small number of fixed categories must leave room for error.

The similarity theory system of assumptions and equations, as derived in this report, defines the relationship between turbulence created by fluxes of heat and momentum, and measured gradients of temperature and wind. The required assumptions are considerably less restrictive than those for the P-T method, and the similarity system of equations presents the minimum amount of information required to adequately specify the relationship between measured profile gradients and turbulence. Because gradients decrease rapidly with height, gradient measurements should be taken at low levels, preferably at 4.0 m.

Turbulence estimates derived by the similarity method from Kansas 1968 Field Program profiles (Izumi, 1971) are accurate, matching measured turbulence values to within 10 percent. The average error increased to 24 percent for uncontrolled meteorological conditions and field grade equipment used at the DPG West Vertical Grid tower. Two types of error were noted in these data sets. The first is a systematic underprediction of  $\sigma_e$  by the similarity method for all except the near neutral turbulence values. Increasing constant B in equation (36) from 1.73 to a value near 1.8 would largely eliminate the systematic error. An interesting consequence of this change is that the balance between  $\epsilon_b$  and  $\epsilon_s$  would occur at  $z/L = 0.35$ , which is equal to von Karman's constant. From equation (19) it is easily seen that when  $z/L = k$ ,  $gFh/\rho c_p T v^3$  equals 1.0, and the balance between buoyancy and  $\tau$  occurs at unity as Obukhov (1971) intended.

The remaining errors in random scatter are due in part to violation of similarity assumptions and in part to lack of temperature measurement accuracy in the DPG tower data. The random error can be reduced to the 10-percent value found with the Kansas field data (Izumi, 1971) by improving instrument quality and data reduction procedures, and by carefully choosing test conditions.

## 10. LIMITATIONS

The similarity theory arguments presented in this report are valid only for neutral through unstable thermal stratification. A corresponding set of equations has been offered for the stable case, but these equations apply only to stabilities less than the critical Richardson number (Ric). Oke (1970) states that beyond the Ric, the atmosphere is not fully turbulent and there may be no definite forms for profiles of wind and temperature. He concludes that a purely empirical approach is needed for estimating fluxes beyond Ric. With clear skies and strong outgoing radiation, nocturnal conditions at DPG almost always exceed Ric and, therefore, do not lend themselves to a similarity theory solution.

Similarity arguments apply only to the vertical component of turbulence. Calder (1966) provided a theoretical demonstration to support observations that the similarity theory cannot be applied to variances of horizontal components of wind velocity. This viewpoint is reinforced by Lumley and Panofsky (1964), and Panofsky et al. (1979). The horizontal components of turbulence can be reasonably obtained only by measurement.

Similarity arguments do not take into account the mechanical dampening of turbulence at the earth's surface. The turbulence spectrum near the ground is distorted by the proximity of a fixed boundary which breaks up large eddies. This effect is particularly noticeable for low frequency, high amplitude eddies which develop during unstable thermal stratification. It is therefore not desirable to apply the similarity theory sigma e calculation method to heights much below 4.0 meters.

Similarity arguments presented in this report apply only to the surface boundary layer. Considerable work has been done to extend the similarity relationship through the depth of the planetary boundary layer. However, this involves scaling with height of the mixing layer, a measurement not presently available at DPG.

## 11. RECOMMENDATIONS

It is recommended that the similarity theory method described herein be used in the following applications:

a. Hazard Prediction. Hazard prediction programs presently require the input of P-T categories. A simple modification of these programs for similarity method computations can improve prediction accuracy if temperature and wind profile data are made routinely available.

b. Test Go/No-Go Criteria. Meteorologists and Project Officers can use stability information as a quantitative means of evaluating the suitability of meteorological conditions for diffusion tests. Tower profile data are presently collected at the rate of one per second by data acquisition systems. Gradients from these data can be used to produce a real-time update of the stability parameter  $z/-L$  for test control. For tests requiring near neutral conditions, a  $z/-L$  less than 0.03 is required. A  $z/-L$  less than or equal to 0.36 may be used as a go/no-go criterion for testing under free convection conditions. Beyond  $z/-L = 0.36$ , buoyancy forces become large and the probability of erratic cloud behavior increases. As  $z/-L$  approaches 1.0, a condition of light and variable wind may occur where the cloud centroid rises off the ground. Go/no-go criteria for diffusion testing can be based on these  $z/-L$  ranges.

c. Test Data Quality Control. Similarity theory equations describe the relationship between turbulence and measured meteorological profiles. With high quality data collected at a site of uniform roughness during quasi-stationary meteorological conditions, the computed turbulence values should be quite accurate. During testing, comparison of calculated and measured turbulence can be made. If a discrepancy in excess of 20 percent is found, then either the equipment is malfunctioning or meteorological conditions are too variable for the collection of a coherent data set.

d. Modeling. Because  $L$  is constant within the surface boundary layer, profile data used to calculate  $L$  at one representative level provides sufficient information for model computation of  $z/L$  over a full range of height within the SBL. Since equation (33) describes  $\sigma_e$  as a function of only  $z/z_0$  and  $z/-L$ , an entire turbulence profile up to heights of 20 or 30 meters can be developed from a single set of lower level gradient measurements. Consequently, improved diffusion modeling within the SBL may be achieved without the requirement for extensive measurements on tall towers.

## APPENDIX A. REFERENCES

1. Businger, J. A., 1973: Turbulent transfer in the atmospheric surface layer. Workshop in Micrometeorology (D. A. Haugen, Ed.), Amer. Meteor. Soc., Boston, MA, 67-100.
2. Businger, J. A., J. C. Wyngaard, Y. Izumi, and E. F. Bradley, 1971: Flux-profile relationships in the atmospheric surface layer. J. Atmos. Sci., 28, 181-189.
3. Calder, K. L., 1966: Concerning the similarity theory of A. S. Monin and A. M. Obukhov for the turbulent structure of the thermally stratified surface layer of the atmosphere. Quart. J. Roy. Meteor. Soc., 92, 141-146.
4. Dyer, A. J., 1961: Measurements of evaporation and heat transfer in the lower atmosphere by an automatic eddy-correlation technique. Quart. J. Roy. Meteor. Soc., 87, 401-412.
5. Dyer, A. J., 1963: The adjustment of profiles and eddy fluxes. Quart. J. Roy. Meteor. Soc., 89, 276-280.
6. Dyer, A. J., and B. B. Hicks, 1970: Flux-gradient relationships in the constant flux layer. Quart. J. Roy. Meteor. Soc., 96, 715-721.
7. Elliott, W. P., 1958: The growth of the atmospheric internal boundary layer. Trans. Amer. Geophys. Union, 39, 1048-1054.
8. Izumi, U., (Ed.) 1971: Kansas 1968 Field Program Data Report. Environm. Res. Pap. No. 379, AFCRL-72-0041, Air Force Cambridge Research Laboratories, Bedford, MA, 73 pp.
9. Kaimal, J. C., H. E. Cramer, F. A. Record, J. E. Tillman, J. A. Businger, and M. Miyake, 1964: Comparison of bivane and sonic techniques for measuring the vertical wind component. Quart. J. Roy. Meteor. Soc., 90, 467-472.
10. Lumley, J. L., and H. A. Panofsky, The Structure of Atmospheric Turbulence. John Wiley and Sons, NY, 1964, 239 pp.
11. Monin, A. S., and A. M. Obukhov, 1954: Basic laws of turbulent mixing in the atmosphere near the ground. Tr. Akad. Nauk SSSR Geofiz. Inst., 151, 163-187.
12. Monin, A. S., and A. M. Yaglom, Statistical Fluid Mechanics: Mechanics of Turbulence Vol. 1. The MIT Press, Cambridge, MA, 1971, 769 pp.
13. Obukhov, A. M. 1971: Turbulence in an atmosphere with a nonuniform temperature. Boundary-Layer Meteor., 2, 7-29.
14. Oke, T. R., 1970: Turbulent transport near the ground in stable conditions. J. Appl. Meteor., 9, 778-786.
15. Panofsky, H. A., R. Lipschutz, and J. Norman, 1979: On characteristics of wind direction fluctuations in the surface layer. Fourth Symposium on Turbulence, Diffusion, and Air Pollution, Amer. Meteor. Soc., Boston, MA, 1-4.

16. Panofsky, H. A., and R. A. McCormick, 1960: The spectrum of vertical velocity near the surface. Quart. J. Roy. Meteor. Soc., 86, 495-503.
17. Pasquill, F., 1961: The estimation of the dispersion of windborne material. Met. Mag., 90, 33-49.
18. Pasquill, F., Atmospheric Diffusion. John Wiley and Sons, NY, 1974, 429 pp.
19. Paulson, C. A., 1970: The mathematical representation of wind speed and temperature profiles in the unstable atmospheric surface layer. J. Appl. Meteor., 9, 857-861.
20. Swinbank, W. C., 1964: The exponential wind profile. Quart. J. Roy. Meteor. Soc., 90, 119-135.
21. Turner, B. D., 1964: A diffusion model for an urban area. J. Appl. Meteor., 3, 83-91.
22. Waldron, A. W., 1977: Turbulence Measurements on a 48-Meter Tower in Desert Terrain. DPG Doc. No. M615A. US Army Dugway Proving Ground, Dugway, UT 84022, 431 pp. (AD-A049036).
23. Waldron, A. W., 1968: A Basis of Modifying the Pasquill Stability Categories for Use at a Desert Site (unpublished).

## APPENDIX B. PROGRAM LISTING

```
$CONTROL USLINIT,NOSOURCE
C PROGRAM SIGECOMP COMPUTES THE UNSTABLE CASE DIMENSIONLESS
C STABILITY PARAMETER Z/-L (ZL), WHERE Z IS HEIGHT IN METERS
C AND L IS THE MONIN-OBUKHOV LENGTH. WIND AND TEMPERATURE
C GRADIENT DATA ARE USED AS INPUT FOR THIS COMPUTATION. Z
C IS THE HEIGHT ABOVE GROUND FOR WHICH WIND AND TEMPERATURE
C GRADIENTS WERE COMPUTED. ZO IS ROUGHNESS LENGTH IN METERS.
C THE PROGRAM USES ZL TO COMPUTE THE VERTICAL WIND ANGLE STAND
C ARD DEVIATION (SIGE) AND COMPARES IT TO A MEASURED VALUE
C (SIGM) BY MEANS OF FRACTIONAL ERROR (FE). PASQUILL-TURNER
C STABILITY CATEGORY SIGMAS (ICAT) ARE ALSO COMPARED TO SIGM AND
C EVALUATED USING FE.
    EXTERNAL ATAN
    DISPLAY "Z=", "ZO="
    ACCEPT Z,ZO
10   CONTINUE
    PI=3.141592654
    DISPLAY "CAT="
    ACCEPT ICAT
    IF(ICAT.EQ.0.) STOP
    IF(ICAT.EQ.1) CSIGE=15.5
    IF(ICAT.EQ.2) CSIGE=10.08
    IF(ICAT.EQ.3) CSIGE=6.7
    IF(ICAT.EQ.4) CSIGE=4.5
    IF(ICAT.EQ.5) CSIGE=2.98
    IF(ICAT.EQ.6) CSIGE=2.0
    DISPLAY "U=,T=,DUDZ=,DTDZ="
    ACCEPT U,T,DUDZ,DTDZ
    E=ALOG(Z/ZO)
    DUDZ=ABS(DUDZ)
    IF(DTDZ.GE.0.0) GO TO 300
C VK IS THE VON KARMAN CONSTANT
    VK=.35
C G IS FORCE OF GRAVITY, M/SEC**2
    G=9.8
    T=T+273.16
    C=-G*Z*DTDZ/(T*U*DUDZ)
C GO THROUGH ITERATIVE PROCEDURE TO FIND Z/-L
C ZL IS Z DIVIDED BY THE UNSTABLE CASE M-O LENGTH, -L
    ZL=.00001
20   PHI=(1.+15.*ZL)**(-.25)
    PSI=2.* ALOG((1.+1./PHI)/2.) + ALOG((1.+1./PHI**2)/2.) - 2.*1ATAN(1./PHI)+PI/2.
    ALPHA=(1.35*(1.+9.*ZL)**.5)/(1.+15.*ZL)**.25
    ZLNEW=C*ALPHA*(E-PSI)
    IF(ABS(ZLNEW-ZL).LT.0.0005) GO TO 50
    ZL=(ZL+ZLNEW)/2.
    GO TO 20
50   ZL=(ZL+ZLNEW)/2.
    PHI=(1.+15.*ZL)**(-.25)
    PSI=2.* ALOG((1.+1./PHI)/2.) + ALOG((1.+1./PHI**2)/2.) - 2.*
```

```

1ATAN(1./PHI)+PI/2.
USTAR=U*VK/(E-PSI)
UBYUSTAR=(E-PSI)/VK
SIGWBYUSTAR=1.3*((1.+15.*ZL)**(-.25)+1.73*ZL)**.33333
SIGE=SIGWBYUSTAR/UBYUSTAR
C CONVERT SIGE FROM RADIANS TO DEGREES.
SIGE=SIGE*180/PI
DISPLAY "SIGE=",SIGE
DISPLAY "SIGE MEAS="
ACCEPT SIGM
FE=(SIGE-SIGM)/( .5*(SIGE+SIGM))
CFE=(CSIGE-SIGM)/( .5*(CSIGE+SIGM))
FERMS=(FE)**2
CFERMS=(CFE)**2
60 WRITE(6,100)
100 FORMAT(' ',1X,'U',5X,'DTDZ',2X,'DUDZ',2X,'CAT',2X,'CSIGE',2X,
1'SIGM',4X,'SIGE',4X,'FE',4X,'FERMS',3X,'CFE',2X,'CFERMS',2X,
1'Z/-L')
      WRITE(6,200)U,DTDZ,DUDZ,ICAT,CSIGE,SIGM,SIGE,FE,FERMS,CFE,
1CFERMS,ZL
200 FORMAT(' ',F5.2,1X,F6.4,1X,F5.4,2X,I1,2X,F5.2,1X,F7.3,1X,F7.3,
11X,F7.3,1X,F5.3,1X,F7.3,1X,F5.3,1X,F7.3)
      WRITE(6,500)
500 FORMAT('0')
GO TO 400
300 DISPLAY "DTDZ GE 0 COMP NOT POSSIBLE"
400 ACCEPT IDUM
GO TO 10
END

```

APPENDIX C. DISTRIBUTUION LIST

<u>Addressee</u>	<u>Copies</u>
Director National Oceanic and Atmospheric Administration Environmental Research Laboratories Boulder, CO 80302	1
Cooperative Institute for Research in Environmental Sciences (CIRES) ATTN: Dr. John C. Wyngaard Boulder, CO 80309	1
Director of Meteorological Systems National Aeronautics and Space Administration Office of Applications (FM) Washington, DC 20546	1
Environmental Protection Agency Division of Meteorology Research Triangle Park, NC 27711	1
Chief Environmental Data Service Atmopsheric Sciences Library Grammax Building ATTN: D821 Silver Spring, MD 20910	1
Commander US Army White Sands Missile Range ATTN: STEW-TE-ER, Technical Library White Sands Missile Range, NM 88002	1
Commander US Army Yuma Proving Ground ATTN: Technical Library Building 2105 Yuma, AZ 85364	1
Head, Atmospheric Research Section National Science Foundation 1800 G Street, NW Washington, DC 20550	1
Department of the Army Project Manager Smoke/Obscurants ATTN: DRCPM-SMK (H. Smalley) Building 324 Aberdeen Proving Ground, MD 21005	1

<u>Addressee</u>	<u>Copies</u>
National Center for Atmospheric Research NCAR Library PO Box 3000 Boulder, CO 80303	1
Commanding Officer Naval Environment Prediction Research Facility ATTN: Library Monterey, CA 93940	1
Director National Science Foundation Atmospheric Sciences Program 1800 G Street, NW Washington, DC 20550	1
Defense Technical Information Center ATTN: DTIC-DDA-2 Cameron Station, Building 5 Alexandria, VA 22314	2
Commander US Army Test and Evaluation Command ATTN: DRSTE-FA Aberdeen Proving Ground, MD 21005	1
Commander Technical Library Chemical Systems Laboratory Aberdeen Proving Ground, MD 21010	1
Acquisitions Section, IRDB-D823 Library and Information Service Division, NOAA 6009 Executive Blvd Rockville, MD 20752	1
The Library of Congress ATTN: Exchange and Gift Division Washington, DC 20540	2
Air Force Geophysics Laboratory ATTN: LYD Hanscom Air Force Base, MA 01731	1
Commander US Air Force Environmental Technical Application Center Scott Air Force Base, IL 62225	1

<u>Addressee</u>	<u>Copies</u>
US Army Research Office ATTN: DRSRO-PP PO Box 12211 Research Triangle Park, NC 27709	1
Commander US Army Dugway Proving Ground ATTN: STEDP-SD -MT-DA-M -MT-DA-L -MT-DA Dugway, UT 84022	1 2 1 2

END

FILMED

9-83

DTIG